

■ Photodegradation

Exploration of the Photodegradation of Naphtho[2,3-*g*]quinoxalines and Pyrazino[2,3-*b*]phenazinesNicole Kolmer-Anderl,^[a] Andreas Kolmer,^[b] Christina M. Thiele,^{*,[b]} and Matthias Rehahn^{*,[a]}

Abstract: Nitrogen-containing polycyclic aromatic hydrocarbons are very attractive compounds for organic electronics applications. Their low-lying LUMO energies points towards a potential use as n-type semiconductors. Furthermore, they are expected to be more stable under ambient conditions, which is very important for the formation of semiconducting films, where materials with high purity are needed. In this study, the syntheses of naphtho[2,3-*g*]quinoxalines and pyrazino[2,3-*b*]phenazines is presented by using reaction conditions, that provide the desired products in high yields, high purity and without time-consuming purification steps. The HOMO and LUMO energies of the compounds are investigated

by cyclic voltammetry and UV/Vis spectroscopy and their dependency on the nitrogen content and the terminal substituents are examined. The photostability and the degradation pathways of the naphtho[2,3-*g*]quinoxalines and pyrazino[2,3-*b*]phenazines are explored by NMR spectroscopy of irradiated samples affirming the large influence of the nitrogen atoms in the acene core on the degradation process during the irradiation. Finally, by identifying the degradation products of 2,3-dimethylnaphtho[2,3-*g*]quinoxaline it is possible to track down the most reactive position in the compound and, by blocking this position with nitrogen, to strongly increase the photostability.

Introduction

Polycyclic aromatic hydrocarbons, like tetracene and pentacene and their derivatives, are of special interest due to their big potential as semiconductors in organic electronic applications, like organic field effect transistors (OFETs).^[1] Especially pentacene as excellent p-type semiconductor and its derivatives are well studied also in terms of reducing LUMO energies by adding electron-withdrawing substituents to generate n-type semiconductors.^[2] But compared to the number of known organic p-type semiconductors only few organic semiconductors with n-type behaviour and good transistor properties are known, although they are needed to create, for example, complementary electronic circuits.^[3]

Unfortunately, polycyclic aromatic hydrocarbons are also known for the photochemical reactions they undergo during irradiation. On the one hand endoperoxide formation is reported for pentacene and tetracene and several derivatives when irradiated in the presence of oxygen.^[4] On the other hand di-

merisation occurs during irradiation without oxygen.^[5] However, this reactivity especially of soluble pentacene and tetracene derivatives is a disadvantage in terms of organic field effect transistor applications where highly purified materials are needed to achieve good performances. Hence, the sensibility towards oxidation of these compounds is a disadvantage with regard to the fabrication of stable organic field effect transistors, especially because quinone compounds are known to act as electronic traps.^[6] That is why new organic semiconductors with an increased durability towards photooxidation and low-lying LUMO energies, that are suitable for n-type semiconductor applications, are needed. For this reason nitrogen-containing acenes are one focus of current research.^[7]

Theoretical studies have already shown that increasing the number of nitrogen atoms in the acene core is an efficient tool to increase the electron affinity, which is advantageous for stable n-type behaviour of organic semiconductors.^[8] In addition, these materials exhibit low LUMO energies, which are necessary for n-type semiconductors, too. Furthermore there are several representatives that show good n-type properties in OFET applications.^[9] UV/Vis measurements indicate that the nitrogen atoms increase the stability of acenes towards the undesirable oxidation process due to its higher electron affinity.^[9,10]

In this paper, we report the synthesis of naphtho[2,3-*g*]quinoxalines and pyrazino[2,3-*b*]phenazines and investigate the influence of the nitrogen content in the tetracene core on the LUMO energies and the stability towards photooxidation. For this purpose the degradation process is studied by NMR spectroscopy and the chemical shifts of products and intermediates are calculated to verify the proposed decomposition pathways.

[a] Dr. N. Kolmer-Anderl, Prof. Dr. M. Rehahn
Ernst-Berl-Institut für Technische und Makromolekulare Chemie
Technische Universität Darmstadt
Alarich-Weiss-Straße 4, 64287 Darmstadt (Germany)
E-mail: M.Rehahn@MC.tu-darmstadt.de

[b] Dr. A. Kolmer, Prof. Dr. C. M. Thiele
Clemens-Schöpf-Institut für Organische Chemie und Biochemie
Technische Universität Darmstadt
Alarich-Weiss-Straße 4, 64287 Darmstadt (Germany)
E-mail: Cthiele@thielelab.de

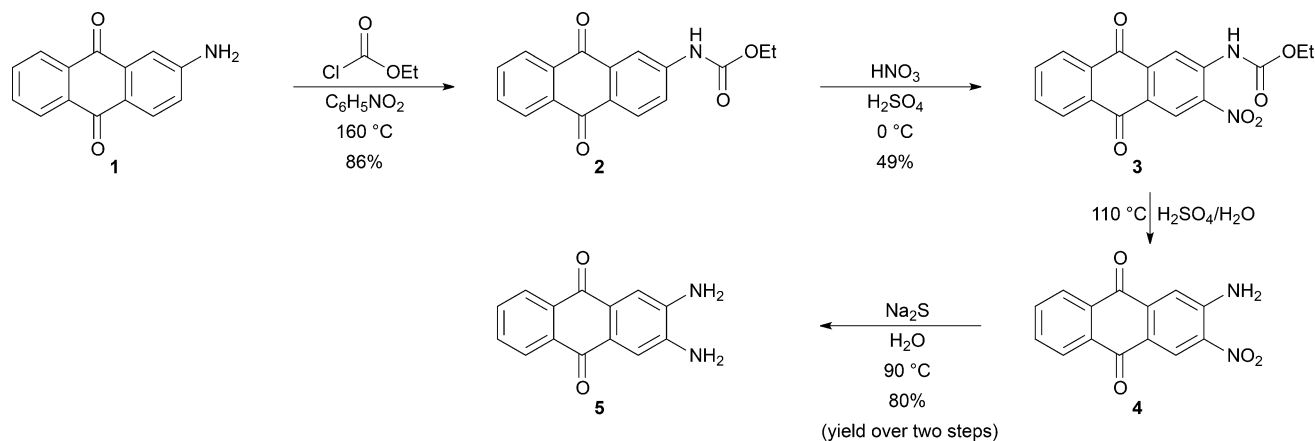
Supporting information for this article is available on the WWW under <http://dx.doi.org/10.1002/chem.201504453>.

Results and discussion

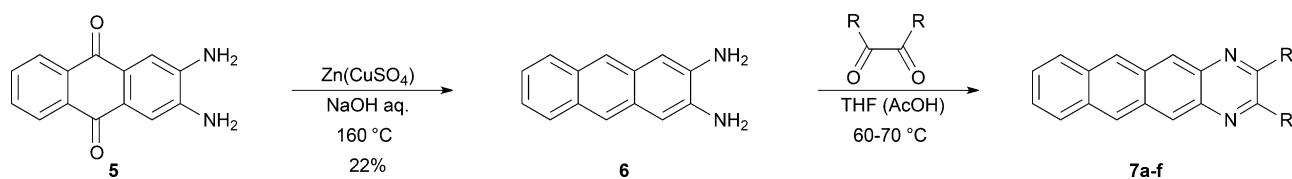
Synthesis

The synthesis of the naphtho[2,3-*g*]quinoxalines **7a–7f** is shown in Schemes 1 and 2. Starting from 2-aminoanthraquinone (**1**), 2,3-diaminoanthraquinone (**5**) was prepared according to the literature procedure of Schaarschmidt and Leu (Scheme 1).^[11] The reduction of 2,3-diaminoanthraquinone (**5**), first reported by Clark,^[12] was modified by using zinc powder, which was activated with an aqueous copper sulphate solution to ensure complete conversion of compound **5** (Scheme 2). Finally, the naphtho[2,3-*g*]quinoxalines **7a–7f** were synthesised from 2,3-diaminoanthracene (**6**) and the corresponding 1,2-diketones (Scheme 2). Except for 1,2-butandione, acetic acid was used as catalyst in the final step of this reaction. Compared to the reaction conditions described by Shitagaki et al.^[13] for the synthesis of phenyl-substituted naphtho[2,3-*g*]quinoxalines, the selected conditions allow a drastic reduction of reaction time from 24 h to 20–50 min. In addition the workup of the reaction mixture is much easier as purification by column chromatography can be avoided, because the raw products can easily be crystallised from toluene (compounds **7c–7f**) or precipitate directly from the reaction mixture (compounds **7a** and **7b**). With this method very good yields can be achieved. The results for the derivatives **7a–7f** are listed in Table 1.

The pyrazino[2,3-*b*]phenazines **9a–9e** were synthesised in analogy to the protocol reported by Armer et al.^[14] 2,3-Diaminophenazine (**8**) was reacted with the appropriate 1,2-diketones (see Scheme 3) but in contrast to the protocol of Armer et al., tetrahydrofuran or methanol were used as solvent instead of pure acetic acid. Only a small amount of acetic acid

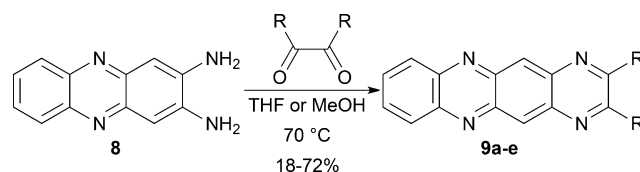


Scheme 1. Synthesis of 2,3-diaminoanthraquinone (**5**) according to Schaarschmidt and Leu.^[11]



Scheme 2. Synthesis of the naphtho[2,3-*g*]quinoxalines **7a–7f**. The reaction conditions and yields for the last step are given in Table 1.

Table 1. Reaction conditions for the synthesis of the naphtho[2,3- <i>g</i>]quinoxaline derivatives 7a–7f .					
	R	AcOH	T [°C]	t [min]	Yield [%]
7a	CH ₃	no	65	20	69
7b	CH ₂ Br	yes	70	20	90
7c	C ₆ H ₅	yes	70	30	88
7d	C ₆ H ₄ F	yes	70	20	36
7e	C ₆ H ₄ Br	yes	60	20	96
7f	C ₆ H ₄ OCH ₃	yes	76	50	77



Scheme 3. Synthesis of the pyrazino[2,3-*b*]phenazines **9a–9e**. The reaction conditions and yields are given in Table 2.

was added to catalyse the reaction leading to the advantage that most of the products precipitate from the reaction mixture and therefore, can be isolated easily with already high purity. Table 2 lists the reaction conditions used and the yields obtained.

Furthermore 2,3-dimethylnaphtho[2,3-*g*]quinoxaline-5,12-dione (**15a**) and 2,3-dimethylnaphtho[2,3-*g*]quinoxaline-6,11-dione (**15b**), which are supposed to be the degradation products of compound **7a**, were synthesised, too (see Schemes 4 and 5). The synthesis of 2,3-dimethylnaphtho[2,3-*g*]quinoxaline-5,12-dione (**15a**) started from 1,4-dimethoxybenzene (**10**),

Table 2. Reaction conditions for the synthesis of the pyrazino[2,3-*b*]phenazine derivatives **9a–9e**.

	R	Solvent	T [°C]	t [min]	Yield [%]
9a	CH ₃	THF	70	120	62
9b	CH ₂ Br	methanol	70	45	18
9c	C ₆ H ₅	methanol	70	360	71
9d	C ₆ H ₄ F	methanol	70	47	72
9e	C ₆ H ₄ CF ₃	methanol	70	30	53

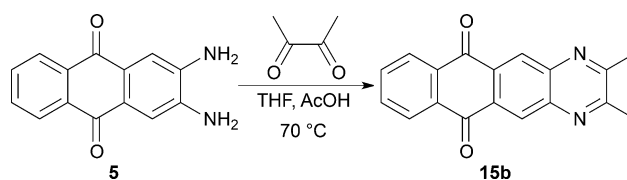
which was converted into 2,3-dimethyl-5,8-dihydroxyquinoxaline (**14**) by a four-step procedure^[15] (see Scheme 4).

As the first step, nitration of 1,4-dimethoxybenzene (**10**) was performed in acetic acid with concentrated nitric acid.^[16] Reduction with H₂/Pd/C in ethyl acetate gave a mixture of compounds **12a** and **12b**.^[17] Separation of the regioisomers was done in the next reaction step. Only compound **12a** gave the quinoxaline **13** during the reaction with 2,3-butanedione, which then could be separated easily from the byproduct **12b**.

Thus, the mixture of compounds **12a** and **12b** was reacted with 2,3-butanedione in acetic acid affording compound **13**, which was transferred into compound **14** by reaction with AlCl₃. Condensation of 2,3-dimethyl-5,8-dihydroxyquinoxaline (**14**) and *o*-phthalaldehyde gave 2,3-dimethylnaphtho[2,3-*g*]quinoxaline-5,12-dione (**15a**) in 70% yield. 2,3-Dimethylnaphtho[2,3-*g*]quinoxaline-6,11-dione (**15b**) was prepared from 2,3-diaminoanthraquinone (**5**) and 2,3-butanedione in THF and acetic acid in 80% yield.

Orbital energies

In order to investigate the influence of the substituents and the nitrogen content on the HOMO and LUMO energies, cyclic voltammetry (CV) and UV/Vis measurements were performed. The HOMO and LUMO levels were obtained from cyclic voltammetry experiments (fully reversible), in dry THF with tetra-*n*-butylammonium hexafluorophosphate (0.1 M) as supporting elec-



Scheme 5. Synthesis of the quinone **15b**, which is supposed to be one of the degradation products of 2,3-dimethylnaphtho[2,3-*g*]quinoxaline (**7a**).

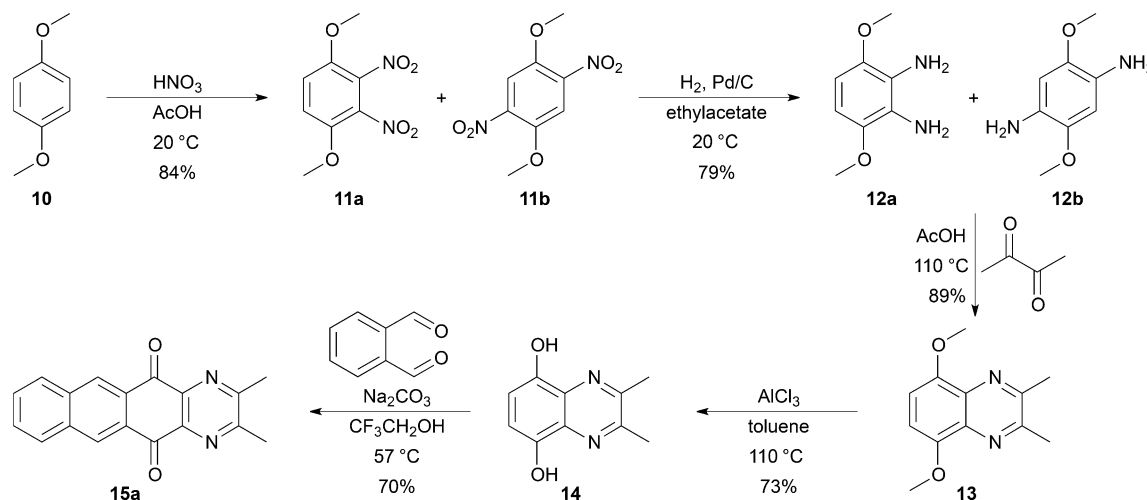
trolyte under a nitrogen atmosphere, by using the formula from de Leeuw et al.^[18] Ferrocene was used as internal standard. If the HOMO energies could not be obtained from cyclic voltammetry measurements, they were also calculated from the LUMO levels and the optical band gap measured by UV/Vis spectroscopy (for more details see the Supporting Information). Compared to compound **7a** the LUMO levels of compounds **7c–7f** are reduced by 0.15–0.24 eV and by 0.65 eV for compound **7b** (Figure 1).

Additionally, phenyl substituents increase the solubility of the products, which is advantageous regarding solution-based applications of the semiconducting film.

Comparing the naphtho[2,3-*g*]quinoxalines **7** and the pyrazino[2,3-*b*]phenazines **9** with the same terminal substituent, the LUMO energies of the pyrazino[2,3-*b*]phenazines are lowered by 0.53 eV for the methyl derivative (i.e., compounds **7a** and **9a**), 0.56 eV for the phenyl derivatives (i.e., compounds **7c** and **9c**) and by 0.61 eV for the fluorophenyl derivatives (i.e., compounds **7d** and **9d**) (Figure 2). From this it follows that the phenyl substituents used affect the energy levels to a lesser extent than the number of nitrogen atoms in the acene core.

Possible degradation pathways and NMR spectroscopic probes thereof

In principle, two degradation pathways for the naphtho[2,3-*g*]quinoxalines and the pyrazino[2,3-*b*]phenazines are expected. On the one hand, photooxidation of one of the non-nitrogen-



Scheme 4. Synthesis of the quinone **15a**, which is supposed to be one of the degradation products of 2,3-dimethylnaphtho[2,3-*g*]quinoxaline (**7a**).

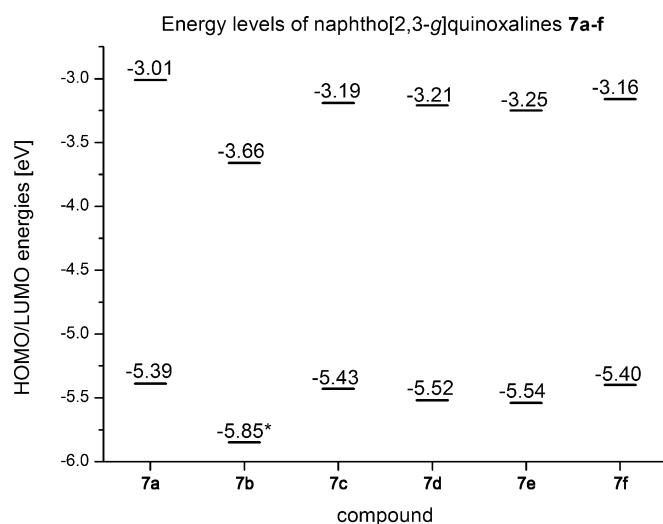


Figure 1. HOMO and LUMO energies of the naphtho[2,3-g]quinoxalines **7a–7f** obtained from cyclic voltammetry measurements in a 0.1 M solution of tetra-*n*-butylammonium hexafluorophosphate in dry THF. Ferrocene was used as internal standard. The value marked with an asterisk is estimated from the LUMO energy obtained from cyclic voltammetry and the optical band gap predicted from UV/Vis measurements (see the Supporting Information). This has been necessary because decomposition of the compound occurred during the cyclic voltammetry measurement.

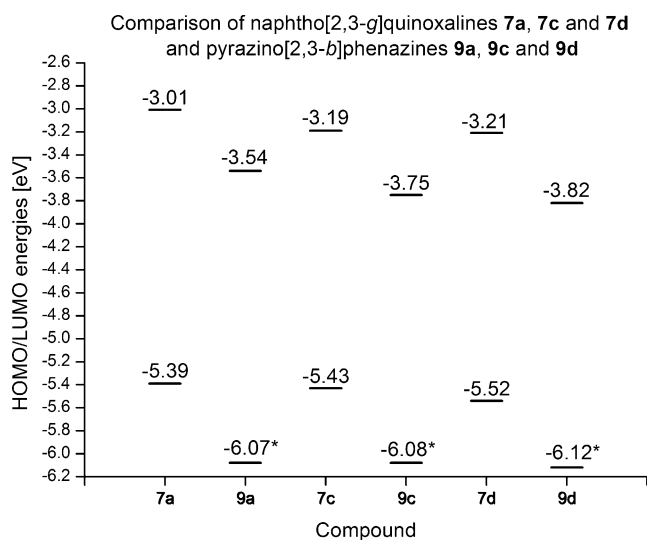


Figure 2. Comparison of the HOMO and LUMO energies of the methyl (i.e., compounds **7a** and **9a**), phenyl (i.e., compounds **7c** and **9c**) and fluoro-phenyl derivatives (i.e., compounds **7d** and **9d**). The values marked with an asterisk are estimated from the LUMO energy obtained from cyclic voltammetry measurements and the optical band gap predicted from UV/Vis measurements (see the Supporting Information).

containing rings could occur, leading to the 2N-quinones **15a**, **15b** or **15c** (see Scheme 6) and to the 4N-quinones **19a** and **19b** (see Scheme 7).

On the other hand, a [4+4] cycloaddition is also possible as a degradation pathway, as this type of reaction is also known from polycyclic aromatic hydrocarbons like tetracene.^[6] In case

of this [4+4] cycloaddition occurring, this leads to the formation of the 2N dimers **17a–17l** (see Figure 3) and to the 4N dimers **20a–20f** (see Figure 4).

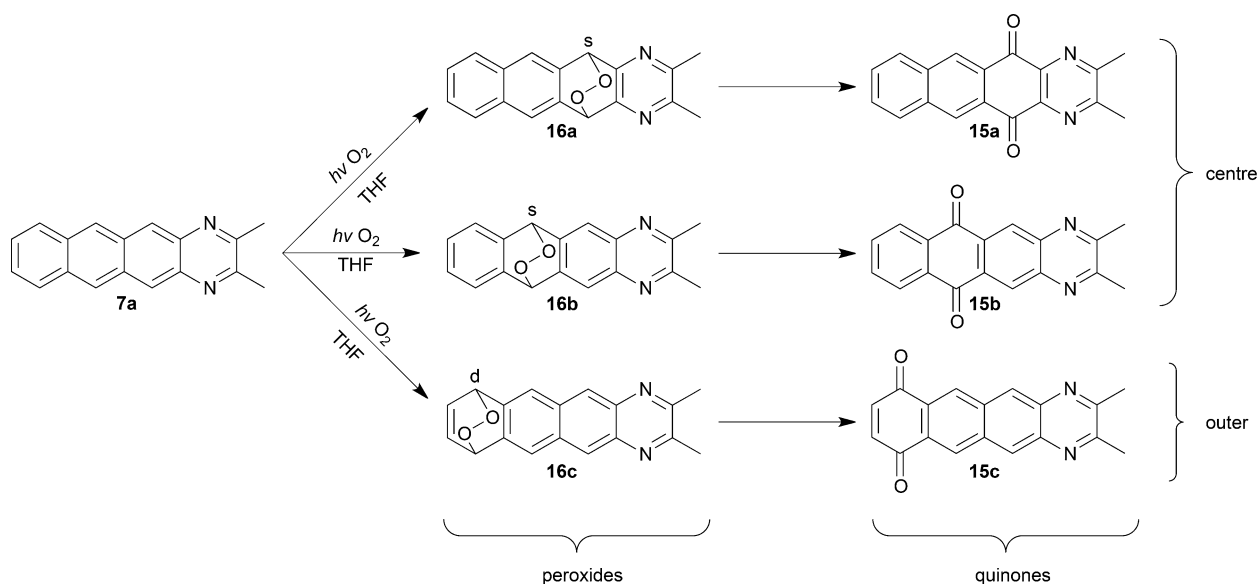
The first question that needs to be addressed is which of the two pathways of degradation is predominant. Thus, to study the degradation of the naphtho[2,3-g]quinoxalines **7** and the pyrazino[2,3-*b*]phenazines **9** NMR measurements were performed. Therefore, saturated solutions (3–4 mg) of the methyl derivatives of the naphtho[2,3-g]quinoxaline **7a** and the pyrazino[2,3-*b*]phenazine **9a** in [D₈]THF (0.5 mL, euriso-top 99.5% D) were irradiated at room temperature and under air in an NMR tube (Norell XR 55) with a 100 W light bulb. After certain time intervals 1D (¹H, ¹³C) and 2D (HSQC, HMBC) NMR spectra were recorded on a Bruker AV-III 600 MHz NMR spectrometer (see the Supporting Information for details) to identify the reactive positions of the molecules **7a** and **9a** and thus gaining insight on the decomposition pathways of the analysed compounds.

To differentiate between the two pathways, it is necessary to identify the decomposition intermediates and products whose signals appear in the recorded NMR spectra. There are two aspects: First, a principal distinction between the appearances of either peroxide, quinone or dimer compounds is needed. Afterwards, in each of those compounds, the reactive position has to be identified.

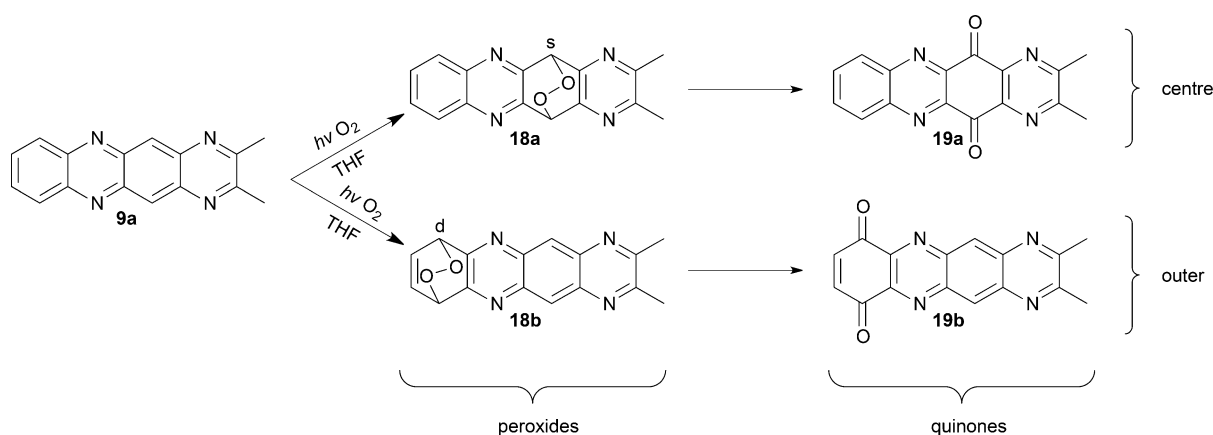
For the first aspect—the differentiation of the decomposition pathways—the chemical shift of the protons and carbon atoms at the bridgehead position and the expected multiplicity (in the ¹H spectra) of the *endo*-peroxides or dimers in each case should be indicative. In terms of chemical shifts one would expect chemical shifts of approximately $\delta = 80$ ppm in the ¹³C spectra for the *endo*-peroxides **16a–16c** and **18a–18b**, whereas for the dimers **17a–17l** and **20a–20f** chemical shifts of approximately $\delta = 50$ ppm in the carbon spectra are expected. Furthermore, it is expected that the peroxide compounds **16** convert into the corresponding 2N-quinones **15** in the course of the photodegradation. The carbonyl ¹³C chemical shifts of these are known to be $\delta = 180.1$ ppm for compound **15a** and $\delta = 181.1$ ppm for compound **15b** as they have been obtained from synthesis for comparison purposes (see above).

In terms of the multiplicity the expected patterns for the bridgehead proton NMR signals are shown in Figures 3 and 4 and Schemes 6 and 7 as denoted by the usual abbreviations (s for singlet, d for doublet, dd for doublet of doublet). As can be seen for both decomposition pathways the expected multiplicities of the bridgehead protons do not allow a distinction between the peroxide and the dimerisation products. In addition, the appearance of various signals for the various possible compounds might lead to an overlap and further complicate the identification and assignment of multiplet structures. Due to the symmetry of most of the compounds, HMBC spectra are not helpful in discriminating between the two pathways.

Thus, to conclude on the possible NMR spectroscopic parameters for the distinction of the two pathways: The only accessible information is the chemical shift of the bridgehead (proton and) carbon atoms. The expected values for the chemical shifts ($\delta = 50$ ppm for dimers, $\delta = 80$ ppm for *endo*-peroxides) are thus backed up with the calculated chemical shifts



Scheme 6. Photooxidation processes of compound **7a** with the proposed nomenclature and the expected multiplicity of the bridgehead protons.



Scheme 7. Photooxidation processes of compound **9a** with the proposed nomenclature and the expected multiplicity for the bridgehead protons.

(see Table 3 in which experimental and calculated chemical shifts for all compounds observed in the following sections are compared). For details on the calculation by using ORCA^[19] and CHESHIRE CCAT^[20] see the Supporting Information. It needs to be pointed out that ¹H chemical shift predictions are not conclusive and are shown here only for comparison with the experimental chemical shifts. From the test set shown in the Supporting Information we can estimate an accuracy of 2 ppm for the calculated ¹³C chemical shifts. Differences of more than 5 ppm are considered interpretable.

Irradiation of 2,3-dimethylnaphtho[2,3-*g*]quinoxaline (**7a**) in the presence of oxygen

First, the investigation of the photodegradation of compound **7a** in the presence of oxygen is studied. A saturated solution of 2,3-dimethylnaphtho[2,3-*g*]quinoxaline (**7a**) (3–4 mg of compound **7a** in 0.5 mL [D₈]THF) was irradiated in one hour steps in the presence of oxygen by a 100 W light bulb to generate

stable conditions for the irradiation process. After every hour ¹H and ¹³C NMR spectra were recorded. In addition, HSQC and HMBC spectra were measured after four and eight hours irradiation time and an additional HMBC spectrum was recorded after ten hours (see Figure 5). Irradiation is continued afterwards. As no decomposition without irradiation has been observed, the time for the NMR experiment does not need to be taken into account.

Figure 5a shows the measured ¹H NMR spectra in which the signal for compound **7a** decreases (green signals) and several additional signals appear during the irradiation process. The most informative signals appearing are the ones of ¹H chemical shifts at $\delta=6.15$ (red signals) and 6.18 ppm (purple signals). These are singlets with the corresponding ¹³C chemical shifts of $\delta=80.1$ and 78.1 ppm, respectively, extracted from the HSQC spectra (Figure 5b). Thus, these signals must belong to the 2N-centre-peroxides **16a** and **16b** (for assignment, which signal set belongs to which compound, see below). Based on the multiplicity, compound **16c** can be excluded (d expected);

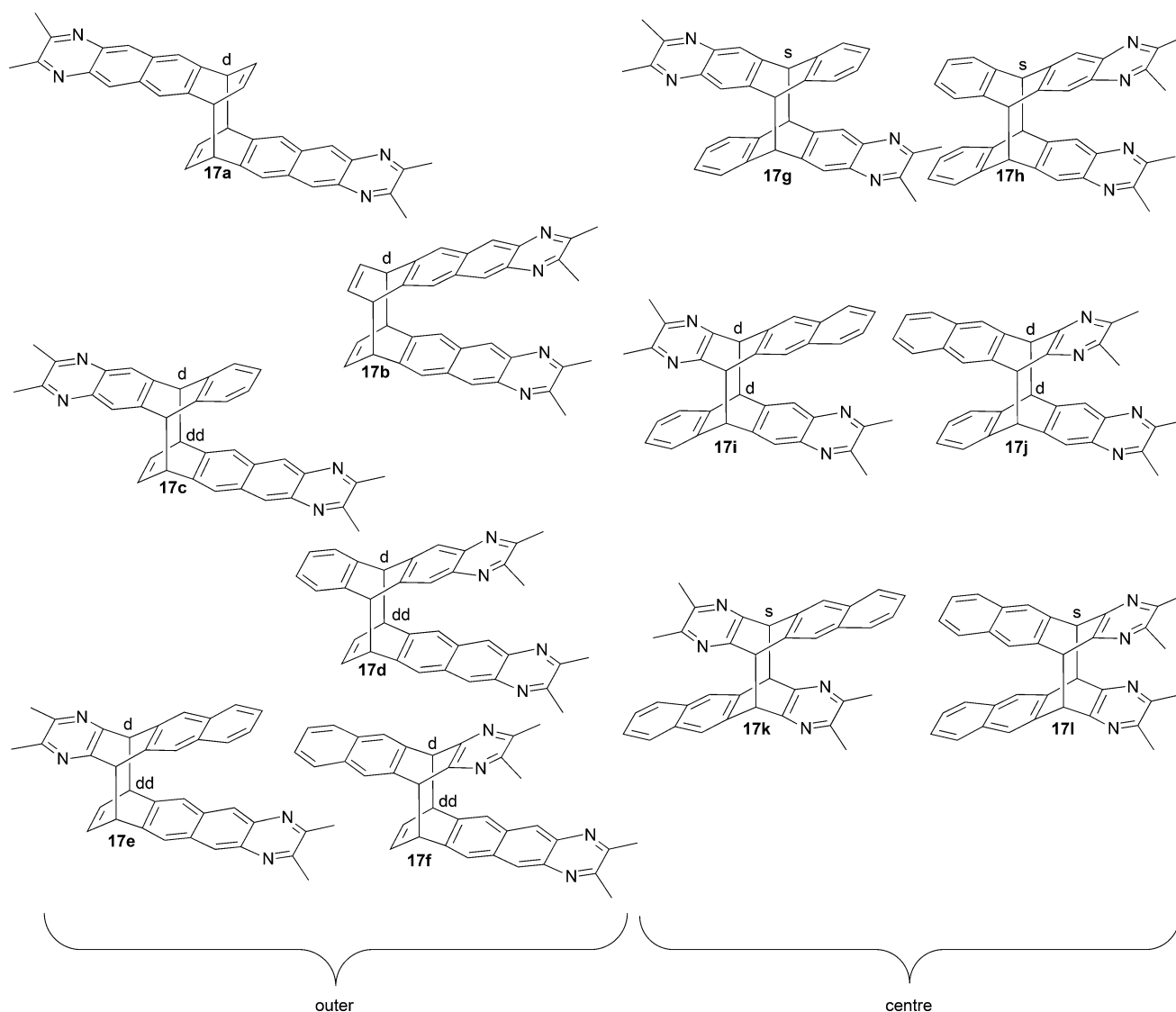


Figure 3. Possible products of the [4+4] photodimerisation of compound **7a** with the expected multiplicity for the bridgehead protons. Each dimer that is formed when one of the outer rings is involved is called 2N-outer-dimer. The ones where only centre rings are involved in the photodimerisation are called 2N-centre-dimers.

this is further confirmed by the calculated chemical shift for the bridgehead carbon atom of compound **16c**, which deviates approximately 6 ppm from the experimentally observed chemical shifts. Also, the dimers can be excluded based on chemical shifts ($\delta \approx 50$ ppm expected). As expected for compounds **16a** and **16b** the ^1H NMR spectrum shows two singlets at $\delta = 6.15$ and 6.18 ppm for the bridgehead protons and two singlets and four doublet doublets (of which the two at $\delta = 7.38$ ppm overlap) in the aromatic region of the spectra. Moreover, the measured chemical shifts of the bridgehead protons are in a very good agreement with the chemical shifts measured for the *endo*-peroxide of tetracene ($\delta = 6.13$ ppm) by Bjarneson and Petersen.^[5]

Additionally, it is seen in the HMBC spectrum after 4 h (Figure 5c) that no correlation to a carbonyl carbon atom is observable yet.

When further irradiating the sample it can be observed, that the signals of compounds **16a** and **16b** start to fade again, whereas new signals appear. These can be assigned to the 2N-quinones **15a** and **15b** (the spectra and assignments of which are known because they were synthesised as compounds for comparison, see above and Table 3). This is also confirmed by the appearance of HMBC correlations in the carbonyl region (see Figure 5d–e). From this it follows that the oxidation of compound **7a** leads to the 2N-centre-peroxides **16a** and **16b** as intermediates and continues to the 2N-centre-quinones **15a** and **15b**.

As can be seen in the spectra, the signals for the *endo*-peroxides **16a** and **16b** do not appear in equal amounts and thus, it would be intriguing to find out, which position is the more reactive one. This is the one that is more prone to oxidation.

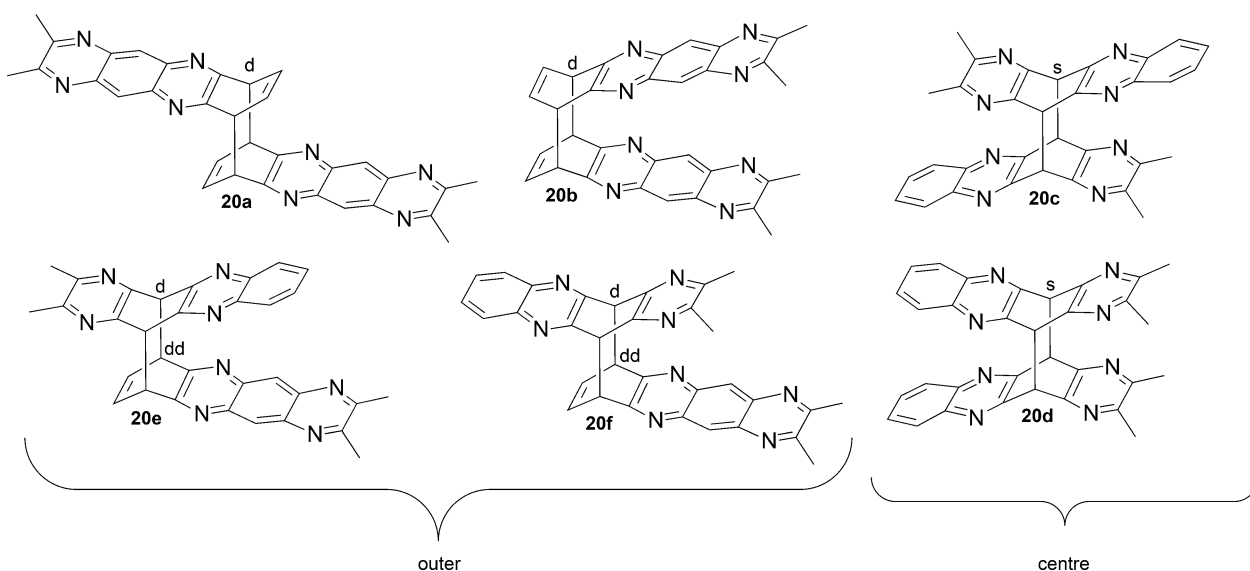


Figure 4. Possible products of the [4+4] photo dimerisation of compound **9a** with the expected multiplicity for the bridgehead protons. Each dimer that is formed when one of the outer rings is involved is called 4N-outer-dimer. The ones where only centre rings are involved in the photodimerisation are called 4N-centre-dimers.

Table 3. A summary of the chemical shifts assigned from the decomposition spectra as shown in Figures 5, 6 and 7 (exptl), calculated chemical shifts (calcd), and experimental chemical shifts of the quinones **15a** and **15b** as synthesised according to Schemes 4 and 5 (synthesised exptl) of the bridge head atoms. For the unsymmetrical dimers **17c**, **17d**, **17e**, **17f**, **17i**, **17j**, **20e** and **20f**, the first value is the one for the “upper” half of the molecule as displayed in the Figures 3 and 4.

	¹ H [ppm]		¹³ C [ppm]		synthesised	¹ H [ppm]		¹³ C [ppm]		
	exptl	calcd	exptl	calcd	exptl	exptl	calcd	exptl	calcd	
16a	6.15	5.33	80.1	79.6	–	18a	6.36	5.08	81.5	81.5
16b	6.18	5.28	78.1	77.8	–	18b	–	4.78	–	76.8
16c	–	4.93	–	74.6	–					
15a	–	–	180.2	177.0	180.1	19a	–	–	178.6	174.9
15b	–	–	181.0	178.5	181.1	19b	–	–	–	178.7
15c	–	–	–	180.7	–					
17a	–	4.38	–	49.7	–	20a	–	4.23	–	48.7
17b	–	4.33	–	51.3	–	20b	–	4.31	–	51.0
17c	–	4.93/4.58	–	55.3/49.9	–	20c	5.35	4.88	51.8	54.0
17d	–	5.08/4.58	–	55.4/50.1	–	20d	5.36	4.88	51.8	54.1
17e	–	4.63/4.53	–	54.7/49.3	–	20e	–	4.53/4.68	–	49.8/54.0
17f	–	4.68/4.53	–	55.1/48.8	–	20f	–	4.50/4.68	–	49.3/53.7
17g	4.83–4.95	5.12	52.0–53.5	54.9	–					
17h	4.83–4.95	5.03	52.0–53.5	55.1	–					
17i	4.83–4.95	4.78/5.03	52.0–53.5	55.0/54.2	–					
17j	4.83–4.95	4.83/5.03	52.0–53.5	55.0/54.2	–					
17k	4.83–4.95	4.92	52.0–53.5	54.1	–					
17l	4.83–4.95	4.83	52.0–53.5	54.3	–					

One could speculate that the *endo*-peroxide **16a** or **16b**, which is formed in a higher amount (purple signals in Figure 5) would also lead to more quinone **15a** or **15b**. This, however, would require that the two respective reaction rates are comparable. With this assumption and the known chemical shifts of compounds **15a** and **15b** one could assign the more abundant quinone to be compound **15b** and thus, the more abundant *endo*-peroxide to be compound **16b** (purple signals in Figure 5). We, however, prefer to have additional spectroscopic evidence for the assignment, which is provided based on correlations in the HMBC spectra, as will be discussed below.

The purple signals in Figure 5 can be related to the 2N-centre-peroxide **16b** because there are two HMBC correlations from the bridgehead carbon atom at $\delta = 78.1$ ppm (¹H chemical shift $\delta = 6.18$ ppm from HSQC) to proton signals at $\delta = 7.38$ (dd) and 7.81 ppm (s) (data not shown). Thus, the bridgehead must be “seeing” two neighbouring (³J(C,H)) protonated carbon atoms with singlet and doublet of doublet multiplicity of the attached protons.

This is expected only for compound **16b**. For compound **16a** only one correlation to a singlet is expected in the HMBC spectrum. This is actually observed: one HMBC correlation

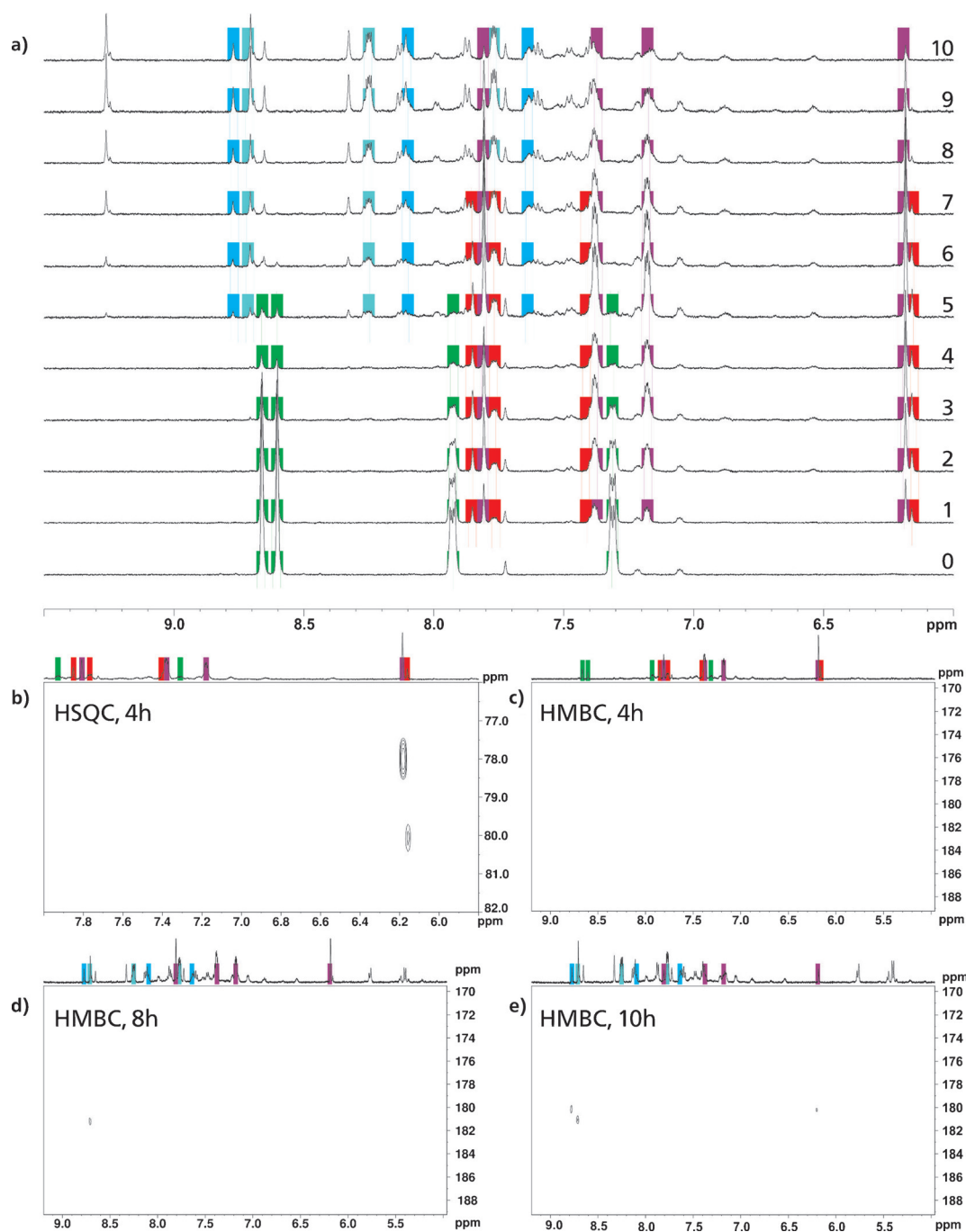


Figure 5. a) ^1H NMR spectra of the irradiation of compound **7a** with light in the presence of oxygen after 0, 1, 2, ..., 10 h in $[\text{D}_6]\text{THF}$. In addition, several 2D NMR experiments were recorded, a selection is shown. The green signals correspond to compound **7a**, the red signals correspond to the 2N-centre-peroxide **16a**, the purple signals correspond to the 2N-centre-peroxide **16b** and the blue signals correspond to the 2N-centre-quinones **15a** and **15b**. b) HSQC spectrum recorded after 4 h of irradiation. The peak at $\delta = 78.1$ ppm, assigned to the 2N-centre-peroxide **16b**, is larger than the one at $\delta = 80.1$ ppm, assigned to the other 2N-centre-peroxide **16a**. c) HMBC spectrum recorded after 4 h of irradiation. There are no peaks in the carbonyl region yet. d) HMBC recorded after 8 h of irradiation. There is one peak in the carbonyl region, which we assigned to the 2N-centre-quinone **15b**. e) HMBC spectrum recorded after 10 h of irradiation. A second peak appears in the carbonyl region, which we assigned to the other 2N-centre-quinone **15a**.

from the bridgehead proton signal (singlet) at $\delta = 6.15$ ppm (^1H , $\delta = 80.1$ ppm for ^{13}C , red signals in Figure 5) to only one other CH carbon atom, which is related through HSQC to a singlet at $\delta = 7.93$ ppm is observed (data not shown).

Hence, the red signals in Figure 5 must belong to the 2N-centre-peroxide **16a**.

As the intensity of the signals of the 2N-centre-peroxide **16b** is larger than the one of the 2N-centre-peroxide **16a**, the corresponding position therefore, should be the most reactive one. Furthermore, there are no signals in the NMR spectra that can be assigned to the 2N-outer-peroxide **16c**. Consequently, this position should be the least reactive.

Irradiation of 2,3-dimethylnaphtho[2,3-*g*]quinoxaline (**7a**) in the absence of oxygen

If oxygen is excluded during the irradiation process, the only degradation pathway left is the dimerisation leading to the compounds **17a–17l**. In the proton spectra of solutions of compound **7a** irradiated in the absence of oxygen, which are shown in Figure 6, several new signals appear at approximately $\delta = 5$ ppm. Their corresponding carbon chemical shifts with $\delta = 52.0\text{--}53.5$ ppm are significantly different from the carbon chemical shifts of the peroxide compounds **16a–16c**. We assume that compounds **17a–17f** are not formed, as the outer ring should also be less reactive in dimerisation reactions. Furthermore, the calculated chemical shifts for the bridgehead carbon atoms in compounds **17a–17f** always include a carbon atom at $\delta = 48\text{--}50$ ppm (not observed) additionally to the one at approximately $\delta = 54$ ppm. The observed ^{13}C chemical shifts of $\delta = 52\text{--}53.5$ ppm are closer to $\delta = 54$ ppm than to $\delta = 48$ ppm, but this observation can only be taken as an indication (as we estimate the accuracy of the calculations to be 2 ppm). As many different dimerisation products are formed and spectra are severely overlapped, multiplicities can only provide a rough guidance. However, if we assume that compounds **17a–17f** are not formed due to the reduced reactivity of the outer ring, one would expect four singlets for the compounds **17g**, **17h**, **17k** and **17l** (symmetric, see Figure 3) and four doublets for the dimers **17i** and **17j** (not symmetric) in the region of $\delta = 5$ ppm. This would lead to twelve lines in this region, which is in good agreement with what is actually observed.

Combining these three indications it can be assumed that the compounds **17g–17l** are the main degradation products of compound **7a**, if oxygen is excluded during the irradiation.

Analysing the degradation spectra after 8 h of irradiation of the oxygen-free sample, it was found that a significant amount

of compound **7a** (approximately 80%) is still left in the sample. In the case of oxygen being present during the irradiation, the signals of compound **7a** disappear already after 5 h of irradiation, showing that oxidation of compound **7a** is faster than dimerisation.

Irradiation of 2,3-dimethylpyrazino[2,3-*b*]phenazine (**9a**) in the presence of oxygen

Once the most reactive position of compound **7a** is known, it can be blocked by two nitrogen atoms to avoid degradation through oxidation of this position, as is the case in 2,3-dimethylpyrazino[2,3-*b*]phenazine (**9a**). In order to prove that this leads to a more stable compound, we tried to prepare a solution of 2,3-dimethylpyrazino[2,3-*b*]phenazine (**9a**) in $[\text{D}_8]\text{THF}$. The solubility of compound **9a** in THF is very limited though (we estimate the concentration of the sample to be 1–2 mg per 0.5 mL). We have nevertheless irradiated the sample in time steps of one hour under the same conditions as used for the solution of 2,3-dimethylnaphtho[2,3-*g*]quinoxaline (**7a**), up to a total irradiation time of 22 h (see the Supporting Information). It was observed that the signals assigned to 2,3-dimethylpyrazino[2,3-*b*]phenazine (**9a**) disappear much slower compared to 2,3-dimethylnaphtho[2,3-*g*]quinoxaline (**7a**) leading to the assumption that 2,3-dimethylpyrazino[2,3-*b*]phenazine (**9a**) is the more stable compound. The novel signals that appeared in the spectrum might be assigned to the dimers **20c** and **20d** because the observed multiplicity is in accordance with the expectation (singlet) and the chemical shifts of these signals are in agreement with what would be expected for these two structures (see Table 3), when assuming that the ^1H chemical shifts of the bridgehead protons would appear at $\delta = 4\text{--}5$ ppm as is the case for the corresponding compounds **17**. However, neither ^{13}C nor HSQC or HMBC spectra can be measured properly due to a low signal intensity.

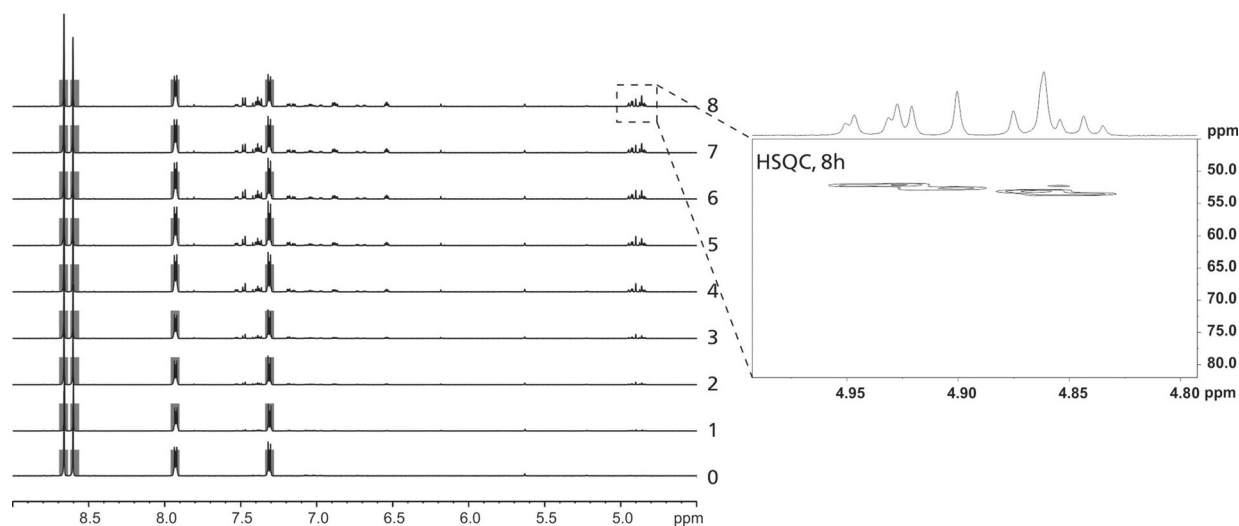


Figure 6. ^1H NMR spectra of the irradiation of compound **7a** with light with exclusion of oxygen after 0, 1, 2, ..., 8 h in $[\text{D}_8]\text{THF}$. The grey signals correspond to compound **7a**. In addition, a HSQC spectrum recorded after 8 h of irradiation is shown, the proton trace of which shows eleven lines. The corresponding carbon atoms possess chemical shifts of $\delta = 52.0\text{--}53.5$ ppm, which indicates that they belong to the 2N-centre-dimers **17g–17l**. No signals can be found in the chemical shift regions where the 2N-peroxides appeared in Figure 5 (^{13}C : $\delta = 75\text{--}80$ ppm).

To gain better information about the degradation process, a saturated solution of 2,3-dimethylpyrazino[2,3-*b*]phenazine (**9a**) in CDCl₃ (3–4 mg of compound **9a** in 0.5 mL CDCl₃) is irradiated under the conditions described above. Here, chloroform is a better solvent for this compound. The recorded ¹H NMR spectra are shown in Figure 7.

Apparently, degradation in CDCl₃ is even slower than in [D₆]THF (despite the higher concentration). Even after a total irradiation time of 61 h approximately 60% of 2,3-dimethylpyrazino[2,3-*b*]phenazine (**9a**) are still present in solution. However, it should be mentioned that during the irradiation process a black precipitate has appeared, which could not be analysed. It is nevertheless possible to measure ¹³C, HSQC and HMBC spectra.

We have conducted the assignment of compounds following the same train of thought as described above in detail for the degradation of compound **7a**.

The situation is different to the one of compound **7a** though: Signals of ¹H chemical shifts at $\delta=5.35/5.36$ ppm (indicative of dimerisation products) and $\delta=6.36$ ppm (indicative of *endo*-peroxides) start to appear at approximately the same time (first signs can be seen after 5 h of irradiation time). Fortunately, the expected number and multiplicity of signals is significantly reduced due to the nitrogen substitution.

From the HSQC spectra, the singlets at $\delta=5.35$ (pink signal in Figure 7) and $\delta=5.36$ ppm (dark pink signal in Figure 7) can be correlated to the carbon signal(s) at $\delta=51.8$ ppm. Due to the observed multiplicity (singlet) and the comparison of the measured and calculated chemical shifts (as listed in Table 3) it seems reasonable to assign these signals to the 4N-centre-

dimers **20c** and **20d**. Looking at the integrals of the appearing signals it can be assumed that the singlet at $\delta=5.35$ ppm and the multiplets at $\delta=7.59$ and 7.88 ppm belong to the same molecule. These values match to the predicted values for compound **20c**.

By using the same arguments, the singlet at $\delta=5.36$ ppm is related to the multiplets at $\delta=7.42$ and 7.72 ppm, which match to the predicted values for compound **20d**.

The singlet at $\delta=6.36$ ppm (brown signal in Figure 7) can be correlated to the carbon signal at $\delta=81.5$ ppm through the HSQC spectrum. Its existence and multiplicity shows that the 4N-centre-peroxide **18a** is present. As additional evidence, the experimental and calculated values for the bridgehead proton and the bridgehead carbon atom are compared, which are in good agreement. There should be more ¹H signals present that belong to compound **18a**, but unfortunately, due to a very low signal intensity and the many overlapping signals the expected multiplets cannot be found/assigned safely.

At longer irradiation times, it is possible to observe signals from the 4N-centre-quinone **19a** (dark red signal in Figure 7). In addition to the measured values for the four aromatic protons (multiplets at $\delta=8.01$ and 8.48 ppm) and the aromatic CH carbon atoms ($\delta=133.4$ and 130.4 ppm) being in very good agreement with the calculated values of this compound, a carbon signal appears at $\delta=178.6$ ppm, which is assigned to the carbonyl group.

From this it follows that the degradation of 2,3-dimethylpyrazino[2,3-*b*]phenazine (**9a**) proceeds through the 4N-centre-peroxide **18a** resulting in the formation of the 4N-centre-quinone **19a**, but is much slower than the oxidation of 2,3-di-

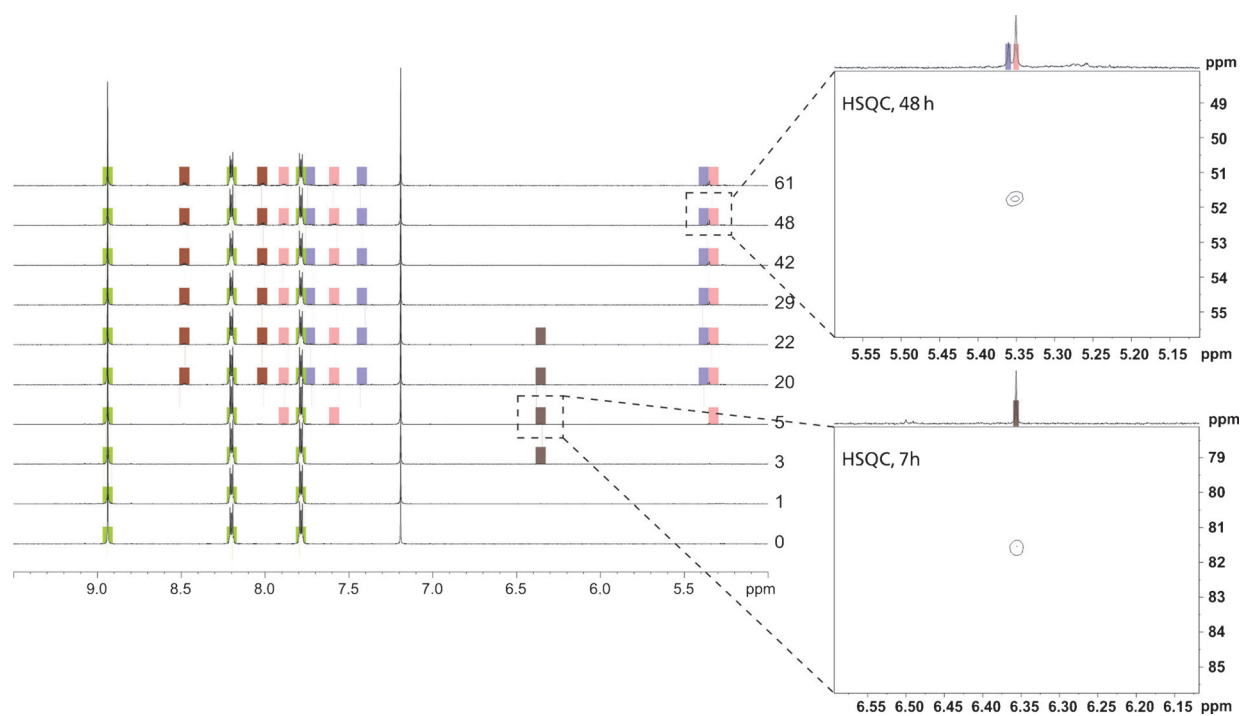


Figure 7. ¹H NMR spectra of the irradiation of compound **9a** with light in the presence of oxygen after 0, 1, 3, 5, 20, 22, 29, 42, 48 and 61 h in CDCl₃. The light green signals correspond to compound **9a**, the brown signals correspond to compound **18a**, the dark red signals correspond to compound **19a** and the pink and dark pink signals correspond to compounds **20c** and **20d**, respectively.

methylnaphtho[2,3-*g*]quinoxaline (**7a**). At the same time the formation of the 4N-centre-dimers **20c** and **20d** in the presence of oxygen is also possible. Furthermore, the degradation in general is much slower, as approximately 60% of compound **18a** are still present after 61 h at a concentration comparable to the ones used before.

Thus, compound **9a** is significantly more stable towards photodegradation as compared to compound **7a**.

Conclusion

Naphtho[2,3-*g*]quinoxalines and pyrazino[2,3-*b*]phenazines have been synthesised in very good yields by the condensation of 2,3-diaminoanthracene or 2,3-diaminophenazine with the appropriate diketones, respectively. The proposed synthetic protocol yields the desired products in high purity so that time-consuming workup like column chromatography and working under inert conditions can be avoided.

This work shows that inserting nitrogen atoms into polycyclic aromatic hydrocarbons is an efficient tool to tune the LUMO energies and to increase the photostability of the products.

Cyclic voltammetry measurements suggest that the LUMO energies are lowered by an increasing nitrogen content independent from the terminal substituents. The terminal substituent does affect the HOMO and LUMO energies as well, but to a minor extent.

By NMR measurements of irradiated samples of 2,3-dimethylnaphtho[2,3-*g*]quinoxaline (**7a**) and 2,3-dimethylpyrazino[2,3-*b*]phenazine (**9a**), it has not only been possible to analyse the dependency of the photostability on the nitrogen content, but also the degradation pathway of compounds **7a** and **9a** has been explored, showing that oxidation is the main degradation pathway.

Elucidation of the degradation products has been used to identify the most reactive position in compound **7a**. Chemical shifts of the expected intermediates and products of the degradation have been predicted, showing a very good agreement with the measured data. In addition the quinones **15a** and **15b** have been synthesised and analysed by NMR spectroscopy. The measured NMR spectra show that these two compounds are the degradation products of compound **7a**. If oxygen is excluded during the irradiation process of compound **7a**, degradation proceeds much slower. The recorded NMR spectra of the oxygen-free samples of 2,3-dimethylnaphtho[2,3-*g*]quinoxaline (**7a**) suggest that in this case dimerisation occurs leading to the compounds **17g**–**17l**.

Subsequently, the CH groups of the most reactive positions in compound **7a** have been substituted by nitrogen atoms leading to compound **9a**, which shows an increased stability compared to compound **7a**. Furthermore, the NMR studies underline that the nitrogen atoms efficiently block the position most susceptible to oxidation of 2,3-dimethylnaphtho[2,3-*g*]quinoxaline. Moreover the studies of compound **9a** indicate that through the decrease in sensitivity towards oxygen the dimerisation process becomes more important.

These results confirm that by adding nitrogen atoms to the acene core it is possible to influence the orbital energies and the compound stability. Moreover, the decomposition to quinone compounds can be drastically reduced by either excluding oxygen or adding nitrogen atoms to the core, thus, reducing the number of potential electronic traps in the material. This opens the opportunity to tailor the properties of organic semiconductors with regard to their application.

Acknowledgements

Generous support from the European Research Council (through 2010-SG_257041), the MerckLab and the Merck KGaA is gratefully acknowledged.

Keywords: degradation pathways · NMR spectroscopy · OFETs · photochemistry · polycyclic aromatic hydrocarbons

- [1] H. Dong, X. Fu, J. Liu, Z. Wang, W. Hu, *Adv. Mater.* **2013**, *25*, 6158–6183.
- [2] Y. Sakamoto, T. Suzuki, M. Kobayashi, Y. Gao, Y. Fukai, Y. Inoue, F. Sato, S. Tokito, *J. Am. Chem. Soc.* **2004**, *126*, 8138–8140.
- [3] H. Usta, A. Fchetti, T. J. Marks, *Acc. Chem. Res.* **2011**, *44*, 501–510.
- [4] J. Reichwagen, H. Hopf, A. Del Guerso, J.-P. Desvergne, H. Bouas-Laurant, *Org. Lett.* **2004**, *6*, 1899–1902; A. G. L. Olive, A. Del Guerso, J.-L. Pozzo, J.-P. Desvergne, J. Reichwagen, H. Hopf, *J. Phys. Org. Chem.* **2007**, *20*, 838–844.
- [5] D. W. Bjarneson, N. O. Petersen, *J. Photochem. Photobiol. A* **1992**, *63*, 327–335.
- [6] J. E. Anthony, *Angew. Chem. Int. Ed.* **2008**, *47*, 452–483; *Angew. Chem.* **2008**, *120*, 460–492.
- [7] U. H. F. Bunz, J. U. Engelhardt, B. D. Lindner, M. Schaffroth, *Angew. Chem. Int. Ed.* **2013**, *52*, 3810–3821; *Angew. Chem.* **2013**, *125*, 3898–3910.
- [8] M. Winkler, K. N. Houk, *J. Am. Chem. Soc.* **2007**, *129*, 1805–1815.
- [9] Z. Liang, Q. Tang, J. Xu, Q. Miao, *Adv. Mater.* **2011**, *23*, 1535–1539.
- [10] G. J. Richards, J. P. Hill, T. Mori, K. Ariga, *Org. Biomol. Chem.* **2011**, *9*, 5005–5017.
- [11] A. Schaarschmidt, H. Leu, *Justus Liebigs Ann. Chem.* **1915**, *407*, 176–194.
- [12] M. Clark, *J. Chem. Soc. C* **1966**, 277–283.
- [13] S. Shitagaki, H. Yamazaki, S. Seo, **2004**, US2005/0003232A1.
- [14] A. M. Amer, A. A. El-Bahnasawi, M. R. H. Mahran, M. Lapib, *Monatsh. Chem.* **1999**, *130*, 1217–1225.
- [15] W. F. Gum, M. M. J. Joullie, *J. Org. Chem.* **1967**, *32*, 53–59.
- [16] F. E. King, N. G. Clark, P. M. H. Davis, *J. Chem. Soc.* **1949**, 3012–3016.
- [17] P. Hammershøj, T. K. Reenberg, M. Pittelkow, C. B. Nielsen, O. Hammerich, J. B. Christensen, *Eur. J. Org. Chem.* **2006**, 2786–2794.
- [18] D. M. de Leeuw, M. M. J. Simenon, A. R. Brown, R. E. F. Einerhand, *Synth. Met.* **1997**, *87*, 53–59; Y. Li, Y. Cao, J. Gao, D. Wang, G. Yu, A. J. Heeger, *Synth. Met.* **1999**, *99*, 243–248; H. Krüger, S. Janietz, D. Sainova, A. Wedel, *Macromol. Chem. Phys.* **2003**, *204*, 1607–1615.
- [19] ORCA—an ab initio, density functional and semiempirical program package, Version 2.8, F. Neese, Max Planck Institut für Bioanorganische Chemie, Mühlheim an der Ruhr (Germany), **2011**; F. Neese, *WIREs Comput. Mol. Sci.* **2012**, *2*, 73–78.
- [20] <http://chenshirenmr.info/>; M. W. Lodewyk, M. R. Siebert, D. J. Tantillo, *Chem. Rev.* **2012**, *112*, 1839; M. W. Lodewyk, D. J. Tantillo, *J. Nat. Prod.* **2011**, *1339*, 1343; R. J. Jain, T. Bally, P. R. Rablen, *J. Org. Chem.* **2009**, *74*, 4017–4023; P. R. Rablen, S. A. Pearlman, J. Finkbiner, *J. Phys. Chem. A* **1999**, *103*, 7357–7363.

Received: November 5, 2015

Published online on February 25, 2016